
Nonlinear vibration analysis of piezolaminated functionally graded cylindrical shell

C.K. Susheel*, Rajeev Kumar and
Vishal Singh Chauhan

School of Engineering,
Indian Institute of Technology Mandi,
Mandi, 175001, Himachal Pradesh, India
Fax: 01905-237945
Email: cksusheel@gmail.com
Email: rajeev.iitmandi@gmail.com
Email: vscitmandi@gmail.com
*Corresponding author

Abstract: In the present work, study of geometric nonlinear vibration analysis of thin piezolaminated functionally graded cylindrical shell is presented. Material properties are graded in the thickness direction of the shell according to power law distribution in terms of volume fraction of the constituents. The shell is modelled using degenerated shell element to predict the deformation under electric voltage and thermal gradient across the thickness of the shell. Modelling is based on the first order shear deformation theory. Second-Piola stress and Green-Lagrange strain tensor are used to perform the large deformation analysis. The accuracy of the developed finite element modelling is validated by comparing numerical results with the published results in the literature. The influence of electric voltage, thermal gradient and gradient index on the vibrational behaviour of cylindrical shell is studied.

Keywords: functionally graded material; FGM; geometric nonlinear; smart structures; vibration control.

Reference to this paper should be made as follows: Susheel, C.K., Kumar, R. and Chauhan, V.S. (2017) 'Nonlinear vibration analysis of piezolaminated functionally graded cylindrical shell', *Int. J. Nonlinear Dynamics and Control*, Vol. 1, No. 1, pp.27–50.

Biographical notes: C.K. Susheel is currently pursuing his PhD degree from Indian Institute of Technology Mandi. He received his MTech from Thapar University Patiala and BTech from National Institute of Technology Jalandhar, India in 2004 and 2008, respectively. His research interests include static and vibration analysis of smart material/structure, finite element method and modelling, control and optimisation.

Rajeev Kumar received his BTech from Institute of Engineering and Technology, CSJM University, Kanpur, MTech from Harcourt Butler Technological Institute (HBTI) Kanpur, and PhD degree from Indian Institute of Technology Roorkee, India in 2000, 2002, and 2008, respectively, all in Mechanical Engineering. He is currently an Assistant Professor at the School of Engineering, Indian Institute of Technology, Mandi, India. His research interests include machine design, solid mechanics, vibration, smart material/structure, finite element method, modelling, control and optimisation.

Vishal Singh Chauhan received his BTech in Mechanical Engineering from Pt. Ravishankar Shukla University Raipur, MTech in Design Engineering from IIT Delhi and PhD degree from Birla Institute of Technology Mesra, Ranchi, India in 1999, 2001, and 2009, respectively. He is currently an Assistant Professor at the School of Engineering, Indian Institute of Technology, Mandi, India. His research interests include design engineering, plastic deformation and fracture of metals and alloys, electromagnetic radiation from metals and alloys, smart materials and structures and mechanical vibration.

1 Introduction

Today's industries, such as automotive, aerospace, electronics and telecommunication and defence, demand best of the properties in a material, like the toughness, electrical conductivity, machinability, low density, high strength, high stiffness, and high temperature resistance. In search of materials with these properties, composite materials and fibre reinforced composite materials were developed. However, due to sudden change in the material properties at the interface of two different materials the problem of debonding takes place at high temperatures. Also, due to difference in the thermal expansion of materials residual stresses occurs which may leads to cracks and hence weaker material section. This leads to generation of materials which overcome these problems and are referred as functionally graded materials (FGMs). The concept of FGM was first proposed in Japan in year 1984. FGM's are isotropic and non-homogeneous and are characterised by the smooth and continuous change of mechanical properties from one surface to the other. FGMs are mostly a mixture of ceramic and metals which are used in thermal environment. Where ceramic constituent provides the resistance to high temperature and the metal (ductile) constituent prevents fracture due to high temperature gradient. The gradation in properties of the material reduces thermal stresses, residual stresses, and stress concentration factors and were exceedingly used as thermal barrier for applications in space planes, space structures, nuclear reactors, turbine rotors, flywheels, gears, and so on (Reddy et al., 2011). Number of researchers has presented analytical and numerical analysis of FGM's over the decade. Reddy (2000) presented both theoretical and finite element analysis of functionally graded (FG) plates based on third order shear deformation theory which accounts for the thermo-mechanical coupling, time dependency and the von Karman-type geometric nonlinearity. Liew et al. (2001) presented the active control of FGM structures using piezoelectric materials. An efficient finite element formulation based on first-order shear deformation theory for static and dynamic piezo-thermo-elastic linear analysis has been used. He et al. (2002) investigated FGMs integrated with piezoelectric sensors and actuators using finite element method for a doubly-curved FGM shell. Both static and dynamic control of FGM shell was performed showing self-controlling and self-monitoring using piezoelectric material. The effectiveness of displacement-cum-velocity feedback control scheme was presented using finite element methods using piezoelectric. An analytical solution was presented by Vel and Batra (2003) for three-dimensional thermo-mechanical deformations of a simply supported FG rectangular plate subjected to time-dependent thermal loads on its top and/or bottom surfaces. Material properties were taken to be analytical functions of the thickness coordinate. The effective elastic moduli at a point are determined by either the

Mori-Tanaka or the self-consistent scheme. Chakraborty et al. (2003) developed a beam element to study thermo-elastic behaviour of FG beam structures which is based on first order shear deformation theory and takes into account the varying elastic and thermal properties along its thickness employing both exponential and power law variation. Qian et al. (2004) used meshless local Petrov-Galerkin method to study free and forced vibrations of FG rectangular plate using higher order shear and normal deformable plate theory. Mori-Tanaka homogenisation technique is used to compute effective material properties. The effect of material properties, boundary conditions and thermal loading on the nonlinear dynamic behaviour of FG plate is studied by Woo et al. (2006). The nonlinear partial differential equations are solved directly with semi analytical method giving solution in terms of mixed Fourier series. A combination of exact and Galerkin method is used for vibration analysis of FG cylindrical shell by Haddadpour et al. (2007). The material properties are graded using simple power law in thickness direction and are also dependent on the temperature. The equations of motion are obtained from Love's shell theory and von Karman-Donnell-type nonlinearity. Kordkheili and Naghdabadi (2007) derived a finite element formulation for geometrically nonlinear thermoelastic analysis of FG plates and shells based on a modified linearisation approach which has resulted from decomposition of the second Piola-Kirchhoff stress and Green-Lagrange strain tensors. An explicit through-the-thickness integral scheme is used to evaluate the force vector and stiffness matrices. A large deformation analysis of FG shells is presented by Arciniega and Reddy (2007) which is based on the first-order shear deformation theory with seven independent parameters where no plane stress assumption is required. To eliminate the effect of membrane shear locking, finite element model is developed using high-order Lagrange elements. A geometrically nonlinear analysis of FGM shells using the element-free kp-Ritz method is presented by Zhao and Liew (2009). The formulation is based on a modified version of Sander's nonlinear shell theory. The nonlinear system equations are solved using arc-length approach along with the Newton-Raphson method. Zhao et al. (2009) studied the static response and free vibration of FGM shells subjected to mechanical or thermo-mechanical loading using the element-free kp-Ritz method. The material properties vary in the thickness direction according to a power-law assumption. The geometric nonlinear static response and free vibration analysis of FG piezoelectric plates under mechanical and electrical loading were also done by Behjat and Khoshnavan (2012) using higher order finite elements. Uymaz and Aydogdu (2013) studied the effects of different material composition and the plate geometry on the critical buckling loads and mode shapes based on small strain elasticity theory with different boundary conditions. The buckling solution is obtained using the Ritz method with Chebyshev polynomials as assumed displacement functions. The vibration behaviour of FG plate is studied by Reddy et al. (2014) analytically using higher order shear deformation theory. Principle of virtual work is used to derive equation of motion and solution is obtained in closed form using Navier's technique.

In this paper, geometrically nonlinear vibration analysis of piezolaminated FG cylindrical shell is presented. A finite element formulation governing the geometrically non-linear electro-thermo-elastic behaviour of piezo-laminated FG materials has been derived using the updated Lagrangian approach. The effects of the temperature, actuator voltage and material composition on the natural frequency of FG cylindrical shell are depicted. The vibration control of cylindrical shell under mechanical and thermal loading is also presented, which shows that the vibration in the FG cylindrical shell can be effectively attenuated by applying appropriate electric voltage using various controllers.

2 FG shell

A FG shell consists of local coordinate system (r, s, t) established on the mid surface of the shell. Thickness ' h ' of the shell is represented in ' t ' direction, where $t = -h/2$ represents the metal rich surface and $t = h/2$ represents the ceramic rich surface of the FG shell. In order to obtain the effective properties of the FGMs, the properties are assumed to vary uniformly from bottom surface to top surface through the thickness according to simple power law distribution which can be given as (He et al., 2002)

$$V = \left(\frac{1}{2} + \frac{z}{h} \right)^n \quad (1)$$

where n is non-negative volume fraction index varies from 0 to ∞ , h is thickness of FGM layer.

The effective properties of complete FGM along the thickness can be expressed as

$$P_{eff}(z) = P_T V_T + P_B V_B \quad (2)$$

$$V_T + V_B = 1 \quad (3)$$

where P_T and P_B are properties of top and bottom layers of FGM respectively, P_{eff} is effective property of FGM, V_T and V_B are volume fractions of material at top and bottom layers respectively. From equations (2) and (3), the variation of properties can be represented as

$$Y(z) = (Y_T - Y_B) \left(\frac{1}{2} + \frac{z}{h} \right)^n + Y_B \quad (4)$$

$$\rho(z) = (\rho_T - \rho_B) \left(\frac{1}{2} + \frac{z}{h} \right)^n + \rho_B \quad (5)$$

$$\alpha(z) = (\alpha_T - \alpha_B) \left(\frac{1}{2} + \frac{z}{h} \right)^n + \alpha_B \quad (6)$$

$$d_{31}(z) = (d_{31T} - d_{31B}) \left(\frac{1}{2} + \frac{z}{h} \right)^n + d_{31B} \quad (7)$$

$$b(z) = (b_T - b_B) \left(\frac{1}{2} + \frac{z}{h} \right)^n + b_B \quad (8)$$

where Y is Young's modulus, ρ is density, α is coefficient of thermal expansion, d_{31} is piezoelectric constant, b is dielectric constant of material. The subscripts T and B represent the property of top and bottom layers respectively. n is volume fraction index, h is thickness of material.

2.1 Constitutive equations for FGM

The constitutive equations representing direct and converse effect of a piezoelectric material can be written as

$$\{S^m\} = [Q]\{\varepsilon^m\} - [e]\{E^m\} - \{\lambda\}\theta \quad (9)$$

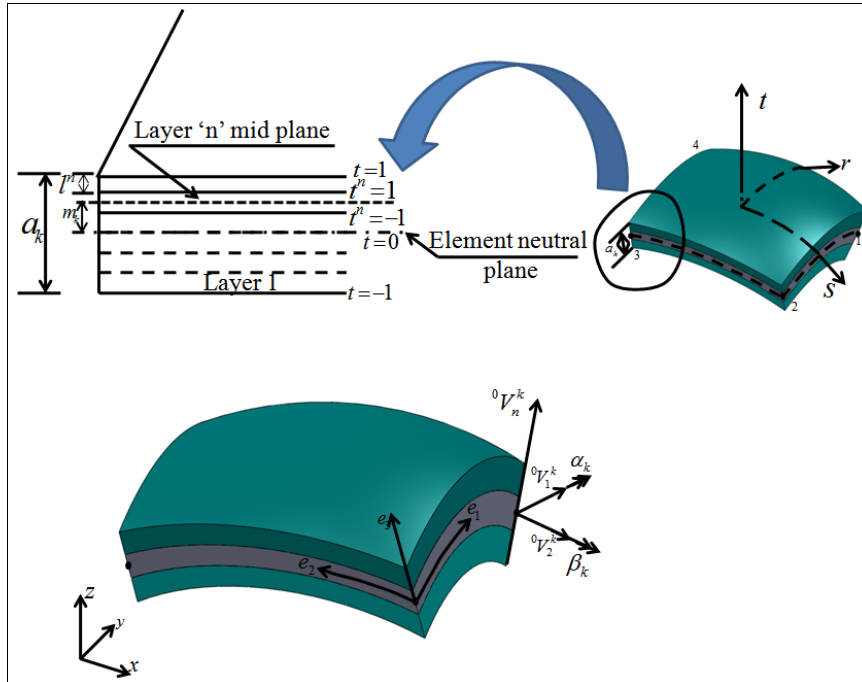
$$\{D^m\} = [e]^T \{\varepsilon^m\} + [b]\{E^m\} + \{P\}\theta \quad (10)$$

where $\{D^m\}$, $\{S^m\}$, $\{\varepsilon^m\}$, $\{E^m\}$ are electric displacement, stress, strain and electric field respectively. ‘ m ’ represents the material coordinate system. $[Q]$, $[e]$ and $[b]$ are the plane-stress reduced elastic stiffness coefficients, the piezoelectric constant matrices respectively. $\{\lambda\}$ and $\{P\}$ are the thermal expansion coefficients and piezoelectric coefficient respectively. θ is the temperature rise from the stress free reference temperature. Equation (9) and equation (10) in matrix form is written in Appendix.

3 Finite element formulation

In the present work, the four noded iso-parametric piezolaminated FG degenerated shell element is used as shown in Figure 1. Figure 1 presents various coordinate systems which are used in the finite element formulation. The main feature of this element is that it is independent of any shell theory and is formulated using three dimensional stress and strain conditions. Element description and basic assumptions used are given in Kumar (2007).

Figure 1 Piezolaminated functionally graded shell element (see online version for colours)



Coordinates of any point within the element can be approximated as

$${}^l x_i(r, s, t) = \sum_{k=1}^4 h_k {}^l x_i^k + \sum_{k=1}^4 \left[\underbrace{\left(-\frac{a_k}{2} + \sum_{i=1}^n l_k^i - \frac{l_k^n}{2} \right)}_{m_k} + t^n \frac{l_k^n}{2} \right] h_k {}^l V_{ni}^k \quad (11)$$

where h_k represents the two dimensional interpolation functions corresponding to node k , given as

- $h_k = \frac{1}{2}(1 \pm r)(1 \pm s)$
- ${}^l x_i$ = global Cartesian coordinates of any point in the element
- ${}^l x_i^k$ = global Cartesian coordinates of nodal point k
- a_k = thickness of shell in t direction at nodal point k , measured along the vector ${}^l V_{ni}^k$
- l_k^i = thickness of layer i at node k
- t^n = natural coordinate of n^{th} layer through the thickness
- m_k = the distance at node k between the element neutral surface and the mid plane of layer n .

Left superscript l has value equal to zero for initial geometry of the element and equal to one for the deformed element geometry.

The displacement of any point within the shell element in the global Cartesian coordinate system is given as

$$u_i(r, s, t) = \sum_{k=1}^4 h_k u_i^k + \sum_{k=1}^4 \left(\left(-\frac{a_k}{2} + \sum_{i=1}^n l_k^i - \frac{l_k^n}{2} \right) + \frac{t^n l_k^n}{2} \right) ({}^0 V_{2i}^k \alpha_k + {}^0 V_{1i}^k \beta_k) \quad (12)$$

where u_i^k are the nodal mid-point displacements in the Cartesian coordinate directions and the α_k and β_k are the rotations of the director vector ${}^0 V_n^k$ about ${}^0 V_1^k$ and ${}^0 V_2^k$ axes respectively.

In compact form the displacement can be written as

$$\{\bar{u}\}_e = \begin{Bmatrix} u \\ v \\ w \end{Bmatrix}_e = [N_{\bar{u}}]_e \{q'\}_e \quad (13)$$

where e represents the element and details of matrices are given in Appendix.

3.1 Strain-displacement relationship

In this study for nonlinear problem it is considered that the displacement is large but the strain is infinitesimal. Also, the conjugate pair of Green-Lagrangian strains and second Piola-Kirchhoff stress tensor is used because the initial configuration is considered as reference configuration. However, if current configuration is considered as reference configuration then the conjugate pairs of Almansi strains and Cauchy stresses should be used. Green-Lagrangian strain is given in Appendix. Strain-displacement relationship can be written in compact form as

$$\begin{aligned} \{ {}_0\varepsilon \}_e &= \{ {}_0e \}_e + \{ {}_0\eta \}_e \\ \{ {}_0\varepsilon \}_e &= [{}_0\bar{B}_L]_e \{ {}_0q' \}_e + [{}_0\bar{B}_{NL}]_e \{ {}_0q' \}_e \end{aligned} \quad (14)$$

where ${}_0e$ and ${}_0\eta$ are the linear and nonlinear strains respectively, $[{}_0\bar{B}_L]_e = [{}_0\bar{B}_{L0}]_e + [{}_0\bar{B}_{L1}]_e$ description of these matrices given in Appendix. $\{ {}_0q' \}_e$ has translation and rotational degree of freedom β_k and α_k , rotational degrees of freedom has been defined in local coordinate system. $\{ {}_0q' \}_e$ can be replaced in equation (14) by the following equation (15) in order to convert rotation degree of freedoms from local coordinate system to global coordinate system. Where $[T_\theta]$ is rotation transformation matrix which is given in Appendix.

$$\{ {}_0q' \}_e = [T_\theta]_e \{ {}_0q \}_e \quad \text{where} \quad \{ {}_0q \}_e = \begin{Bmatrix} \{ {}_0q \}_1 \\ \{ {}_0q \}_2 \\ \{ {}_0q \}_3 \\ \{ {}_0q \}_4 \end{Bmatrix} \quad (15)$$

In the analysis of thin structures, the pure displacement-based plate and shell elements without higher order terms exhibits very stiff behaviour, which is generally referred to as element locking. This stiffness in thin structures is due to the fact that with pure displacement based interpolations the transverse shear strains cannot vanish at all points in the element, when it is subjected to constant bending moment. In order to arrive at efficient non-locking element various procedures has been proposed such as selective and reduced integration, mixed interpolation of displacements and transverse shear strains. Here in this work later procedure is used as given by Dvorkin and Bathe (1984).

Equation (14) can be written after including mixed interpolation of displacement and transverse shear strains as

$$\{ {}_0\varepsilon \}_e = ([{}_0B_L] + [{}_0B_{NL}]) \{ {}_0q' \}_e \quad (16)$$

substituting equation (15) in equation (16) and equation (13) we get

$$\{ {}_0\varepsilon \}_e = ([{}_0B_L] + [{}_0B_{NL}]) [T_\theta]_e \{ {}_0q \}_e \quad (17)$$

$$\{ {}_0\varepsilon \}_e = [{}_0B_L] [T_\theta]_e \{ {}_0q \}_e + [{}_0B_{NL}] [T_\theta]_e \{ {}_0q \}_e = {}_0e + {}_0\eta \quad (18)$$

$$\{ {}_0\bar{u} \}_e = [N_{\bar{u}}]_e [T_\theta]_e \{ {}_0q \}_e \quad (19)$$

3.2 Electric field

The electric field is assumed to be constant within the element. Also, it is assumed that the electric field acts in the thickness direction of the piezoelectric layers. Such formulation gives one electric degree of freedom per layer per element for the electric field. Electric field inside the i^{th} layer within the element can be given mathematically as:

$$\{ {}_0 E \}_n = -\{ {}_0 B_\varphi \}_e \{ {}_0 \varphi_{p_n} \} \quad (20)$$

where

$$\{ {}_0 B_\varphi \}_e = \frac{1}{t_{p_n}} \begin{Bmatrix} V_{31} \\ V_{32} \\ V_{33} \end{Bmatrix} \quad (21)$$

V_{31} , V_{32} and V_{33} are the direction cosines of normal unit vector V_3 at node k and t_{p_n} and ${}_0 \varphi_{p_n}$ are the thickness and electric potential of n th piezoelectric layer.

3.3 Temperature field

The temperature distribution is assumed to be linear within the element. Using the shape functions, the temperature of any point in the element can be uniquely given in terms of nodal temperature ' Θ ' and the temperature gradient ' φ ' of the mid plane as:

$$\{ {}_0 \Theta \}_e = [N_\Theta]_e \{ {}_0 \theta \}_e + [N_\varphi]_e \{ {}_0 \theta \}_e \quad (22)$$

where

$$\begin{aligned} [N_\Theta] &= [h_k \quad 0] \\ [N_\varphi] &= [0 \quad h_k H] \\ \{ \theta \} &= \begin{Bmatrix} \Theta \\ \varphi \end{Bmatrix} \end{aligned} \quad (23)$$

To obtain the electric displacement $\{D\}$ and stress $\{\sigma\}$ using the constitutive equations (9) and (10), the strain, temperature and electric field given by equations (18), (20) and (22) can be used. The constitutive equations defined are in material coordinate system, whereas the strain, temperature and electric field are defined in the global coordinate system. Thus, the constitutive equations must be first transferred into local coordinate system and then to global coordinate system. This can be achieved with the help of transformation matrices which are given in the Appendix.

Therefore, the constitutive equations after transformation into global coordinates can be written as

$$\begin{aligned} \{ {}_0 \sigma \} &= [T_\varepsilon]^T [T_o]^T [Q][T_o][T_\varepsilon] \{ {}_0 \varepsilon \} - [T_\varepsilon]^T [T_o]^T [e]^T [T_v] \{ {}_0 E \} \\ &\quad - [T_\varepsilon]^T [T_o]^T [\lambda][T_o] \{ {}_0 \theta \} \end{aligned} \quad (24)$$

$$\{ {}_0 D \} = [T_v]^T [e][T_o][T_e]\{ {}_0 \varepsilon \} + [T_v]^T [b][T_v]\{ {}_0 E \} + [T_v]^T [p]\{ {}_0 \theta \} \quad (25)$$

In condensed form it can be written as

$$\{ {}_0 \sigma \} = [\bar{Q}]\{ {}_0 \varepsilon \} - [\bar{e}]^T \{ {}_0 E \} - \{ \bar{\lambda} \} \{ {}_0 \Theta \} \quad (26)$$

$$\{ {}_0 D \} = [\bar{e}]\{ {}_0 \varepsilon \} + [\bar{b}]^T \{ {}_0 E \} + \{ \bar{p} \} \{ {}_0 \Theta \} \quad (27)$$

3.4 Potential energy

In a piezolaminated FG shell element the potential energy consists of strain energy and electric energy is given as (Tanveer and Singh, 2010)

$$U = \int_{0V} \left(\frac{1}{2} {}^{t+\Delta t} \bar{\varepsilon}^T {}^{t+\Delta t} \bar{S} - \frac{1}{2} {}^{t+\Delta t} \bar{E}^T {}^{t+\Delta t} \bar{D} \right) d^0V \quad (28)$$

where the left subscript represents the configuration w.r.t. which the different variables are defined and the left superscript represent the configuration at which the different variables are to be calculated.

The converse and direct constitutive equations w.r.t. configuration at time $t + \Delta t$ can be written as

$${}^{t+\Delta t} \bar{S} = Q {}^{t+\Delta t} \bar{\varepsilon} - e^T {}^{t+\Delta t} \bar{E} - \lambda {}^{t+\Delta t} \bar{\Theta} \quad (29)$$

$${}^{t+\Delta t} \bar{D} = e {}^{t+\Delta t} \bar{\varepsilon} + b {}^{t+\Delta t} \bar{E} + p {}^{t+\Delta t} \bar{\Theta} \quad (30)$$

Substituting equations (29) and (30) in equation (28) we get

$$U = \int_{0V} \left(\frac{1}{2} {}^{t+\Delta t} \bar{\varepsilon}^T \left(\bar{Q} {}^{t+\Delta t} \bar{\varepsilon} - \bar{e}^T {}^{t+\Delta t} \bar{E} - \bar{\lambda} {}^{t+\Delta t} \bar{\Theta} \right) - \frac{1}{2} {}^{t+\Delta t} \bar{E}^T \left(\bar{e} {}^{t+\Delta t} \bar{\varepsilon} + \bar{b} {}^{t+\Delta t} \bar{E} + \bar{p} {}^{t+\Delta t} \bar{\Theta} \right) \right) d^0V \quad (31)$$

The strain, temperature and electric field can be divided into two parts, known part and incremental part, i.e.

$${}^{t+\Delta t} \bar{\varepsilon} = {}^t \bar{\varepsilon} + {}_0 \bar{\varepsilon}, \quad {}^{t+\Delta t} \bar{E} = {}^t \bar{E} + {}_0 \bar{E} \quad \text{and} \quad {}^{t+\Delta t} \bar{\Theta} = {}^t \bar{\Theta} + {}_0 \bar{\Theta} \quad (32)$$

Also,

$$\delta {}^{t+\Delta t} \bar{\varepsilon} = \delta {}_0 \bar{\varepsilon}, \quad \delta {}^{t+\Delta t} \bar{E} = \delta {}_0 \bar{E} \quad \text{and} \quad \delta {}^{t+\Delta t} \bar{\Theta} = \delta {}_0 \bar{\Theta} \quad (33)$$

Further, the strain tensor can be split into linear and nonlinear part as

$${}_0 \bar{\varepsilon} = {}_0 \bar{e} + {}_0 \bar{\eta} \quad (34)$$

Taking variation of equation (31) and using equations (32), (33) and (34) we get

$$\begin{aligned}
\delta U = & \int_{0_V} \delta_0 \bar{e}^T \bar{Q}_0 \bar{e} d^0 V + \int_{0_V} \delta_0 \bar{e}^T \bar{t}_0 \bar{S} d^0 V + \int_{0_V} \delta_0 \bar{\eta}^T \bar{t}_0 \bar{S} d^0 V \\
& - \int_{0_V} \delta_0 \bar{E}^T \bar{e}_0 \bar{\varepsilon} d^0 V - \int_{0_V} \delta_0 \bar{E}^T \bar{e}_0 \bar{e} d^0 V + \int_{0_V} \delta_0 \bar{E}^T \bar{b}_0 \bar{E} d^0 V \\
& - \int_{0_V} \delta_0 \bar{e}^T \bar{e}^T \bar{e}_0 \bar{E} d^0 V - \int_{0_V} \delta_0 \bar{\eta}^T \bar{e}^T \bar{e}_0 \bar{E} d^0 V \\
& + \frac{1}{2} \left\{ \int_{0_V} \delta_0 \bar{\Theta}^T \bar{\lambda}_0 \bar{\varepsilon} d^0 V + \int_{0_V} \delta_0 \bar{\Theta}^T \bar{\lambda}_0 \bar{e} d^0 V + \int_{0_V} \delta_0 \bar{e}^T \bar{\lambda}_0 \bar{\Theta} d^0 V \right. \\
& \quad + \int_{0_V} \delta_0 \bar{e}^T \bar{\lambda}_0 \bar{\Theta} d^0 V - \int_{0_V} \delta_0 \bar{\Theta}^T \bar{p}_0 \bar{E} d^0 V - \int_{0_V} \delta_0 \bar{\Theta}^T \bar{p}_0 \bar{E} d^0 V \\
& \quad \left. - \int_{0_V} \delta_0 \bar{E}^T \bar{p}_0 \bar{\Theta} d^0 V - \int_{0_V} \delta_0 \bar{E}^T \bar{p}_0 \bar{\Theta} d^0 V \right\} \tag{35}
\end{aligned}$$

Now substituting from equations (18), (19), (20) and (22) into (35)

$$\begin{aligned}
\delta U = & \int_{0_V} \{\delta q\}_e^T [T_\theta]_e^T [B_L]_e^T [\bar{Q}] [B_L]_e [T_\theta]_e \{q\}_e d^0 V \\
& + \int_{0_V} \{\delta q\}_e^T [T_\theta]_e^T [B_L]_e^T \{t_0 S\} d^0 V \\
& + \int_{0_V} \{\delta q\}_e^T [T_\theta]_e^T [B_{NL}]_e^T \{t_0 S\} [B_L]_e [T_\theta]_e \{q\}_e d^0 V \\
& - \int_{0_V} \{\delta \phi_n\}_e^T \{B_\phi\}_e^T [\bar{e}] \{t_0 \varepsilon\}_e d^0 V - \int_{0_V} \{\delta \phi_n\}_e^T \{B_\phi\}_e^T [\bar{e}] [B_L]_e [T_\theta]_e \{q\}_e d^0 V \\
& - \int_{0_V} \{\delta \phi_n\}_e^T \{B_\phi\}_e^T [\bar{b}] \{t_0 E\}_e d^0 V - \int_{0_V} \{\delta \phi_n\}_e^T \{B_\phi\}_e^T [\bar{e}] \{B_\phi\}_e \{\phi_n\}_e d^0 V \\
& - \int_{0_V} \{\delta q\}_e^T [T_\theta]_e^T [B_L]_e^T [\bar{e}]^T \{B_\phi\}_e \{\phi_n\}_e d^0 V \\
& - \int_{0_V} \{\delta q\}_e^T [T_\theta]_e^T [B_{NL}]_e^T \{\bar{e}^T t_0 E\} [B_L]_e [T_\theta]_e \{q\}_e d^0 V \\
& + \frac{1}{2} \int_{0_V} \{\delta \theta\}_e^T [N_\theta]_e^T [\bar{\lambda}] \{t_0 \varepsilon\}_e d^0 V + \frac{1}{2} \int_{0_V} \{\delta \theta\}_e^T [N_\theta]_e^T [\bar{\lambda}] [B_L]_e [T_\theta]_e \{a\}_e d^0 V \\
& + \frac{1}{2} \int_{0_V} \{\delta q\}_e^T [T_\theta]_e^T [B_L]_e^T [\bar{\lambda}] \{t_0 \theta\}_e d^0 V \\
& + \frac{1}{2} \int_{0_V} \{\delta q\}_e^T [T_\theta]_e^T [B_L]_e^T [\bar{\lambda}] [N_\theta]_e \{\theta\}_e d^0 V \\
& - \frac{1}{2} \int_{0_V} \{\delta \theta\}_e^T [N_\theta]_e^T [\bar{p}] \{t_0 E\}_e d^0 V - \frac{1}{2} \int_{0_V} \{\delta \theta\}_e^T [N_\theta]_e^T [\bar{p}] \{B_\phi\}_e \{\phi_n\}_e d^0 V \tag{36} \\
& - \frac{1}{2} \int_{0_V} \{\delta \phi_n\}_e^T \{B_\phi\}_e^T [\bar{p}] \{t_0 \theta\}_e d^0 V - \frac{1}{2} \int_{0_V} \{\delta \phi_n\}_e^T \{B_\phi\}_e^T [\bar{p}] [N_\theta]_e \{\theta\}_e d^0 V
\end{aligned}$$

$$\begin{aligned}
 \delta U = \{ \delta_0 q \}_e^T & \left\{ [K_L] \{ q \}_e + [K_{NL}] \{ q \}_e - [H_{NL}] \{ q \}_e + \{ {}^t_0 F \}_e \right. \\
 & \left. - [K_{u\phi}] \{ \phi_{pn} \}_e + \{ F_{u\theta} \}_e + \frac{1}{2} [K_{u\theta}] \{ \theta \}_e \right\} \\
 & + \{ \delta \phi_{pn} \}_e \left\{ - [K_{\phi u}] \{ q \}_e - [K_{\phi\phi}] \{ \phi_{pn} \}_e - \{ F_{\phi u} \}_e \right. \\
 & \left. - \{ F_{\phi\phi} \}_e - \{ F_{\phi\theta} \}_e - \frac{1}{2} [K_{\phi\theta}] \{ \phi_{pn} \}_e \right\} \\
 & + \{ \delta \theta \}_e^T \left\{ \frac{1}{2} [K_{\theta u}] \{ q \}_e - \frac{1}{2} [K_{\theta\phi}] \{ \phi_{pn} \}_e + \frac{1}{2} \{ F_{\theta\phi} \}_e + \{ F_{\theta u} \}_e \right\}
 \end{aligned} \quad (37)$$

3.5 Kinetic energy

$$T = \frac{1}{2} \int_{0^V} \rho \{ \dot{\bar{u}} \}^T \{ \dot{\bar{u}} \} d^0V \quad (38)$$

where ρ is the density. Now by using equation (28) we get

$$T = \frac{1}{2} \int_{0^V} \rho \{ \dot{q} \}_e^T [T_\theta]_e^T [N_{\bar{u}}]_e^T [N_{\bar{u}}]_e [T_\theta]_e \{ \dot{q} \}_e d^0V \quad (39)$$

$$T = \frac{1}{2} \int_{0^V} \{ \dot{q} \}_e^T [M_{uu}] \{ \dot{q} \}_e d^0V \quad (40)$$

$$\delta T = \{ \dot{q} \}_e^T [M_{uu}] \{ \dot{q} \}_e \quad (41)$$

3.6 Work potential by the external forces and electrical charge

$$W_{ext} = \int_{0^V} \{ \bar{u} \}_e^T \{ F_b \}_e d^0V + \int_{0^S} \{ \bar{u} \}_e^T \{ F_S \}_e d^0S + \{ \bar{u} \}_e^T \{ F_p \}_e - \int_{0^S} \{ E \}_e^T \{ F_q \}_e d^0S \quad (42)$$

where $\{ F_b \}$, $\{ F_S \}$, $\{ F_p \}$ and $\{ F_q \}$ are body force, surface force, point force and surface electrical charge density respectively. Now using equations (19) and (20) in (42) we get

$$\begin{aligned}
 W_{ext} = \int_{0^V} \{ q \}_e^T [T_\theta]_e^T [N_{\bar{u}}]_e^T \{ F_b \}_e d^0V + \int_{0^S} \{ q \}_e^T [T_\theta]_e^T [N_{\bar{u}}]_e^T \{ F_S \}_e d^0S \\
 + \{ q \}_e^T [T_\theta]_e^T [N_{\bar{u}}]_e^T \{ F_p \}_e + \int_{0^S} \{ \phi \}_e^T \{ B_\phi \}_e^T \{ F_q \}_e d^0S
 \end{aligned} \quad (43)$$

$$W_{ext} = \{ q \}_e^T \{ F_m \}_e + \{ \phi \}_e^T \{ F_q \}_e \quad (44)$$

$$\delta W_{ext} = \{ \delta q \}_e^T \{ F_m \}_e + \{ \delta \phi \}_e^T \{ F_q \}_e \quad (45)$$

3.7 Equation of motion

Using the Hamilton's principle the equation of motion for the piezolaminated shell element can be written as

$$\int_{t_1}^{t_2} (\delta T - \delta U + \delta W_{ext}) dt = 0 \quad (46)$$

where T , U and W_{ext} represents the kinetic energy, potential energy and work done by external forces respectively. δ is the variational operator, t_1 and t_2 are arbitrary time values.

Now substituting (37), (41) and (45) in equation (46) we get

$$\left(\int_{t_1}^{t_2} \{\delta q\}_e^T \left(-[M_{uu}]_e \{\ddot{q}\}_e - \begin{pmatrix} [K_L]\{q\}_e + [K_{NL}]\{q\}_e - [H_{NL}]\{q\}_e + \{^t_0 F\}_e \\ -[K_{u\phi}]\{\phi_{p_n}\}_e + \{F_{u\theta}\}_e + [K_{u\theta}]\{\theta\}_e - \{F_{u\theta}\}_e + \{F_m\}_e \end{pmatrix} \right) \right. \\ \left. + \int_{t_1}^{t_2} \{\delta \phi_{p_n}\}_e^T \left([K_{\phi u}]\{q\}_e + [K_{\phi\phi}]\{\phi_{p_n}\}_e + \{F_{\phi u}\}_e + \{F_{\phi\phi}\}_e \right) \right. \\ \left. + \int_{t_1}^{t_2} \{\delta \theta\}_e^T \left([K_{\phi\theta}]\{\phi_{p_n}\}_e + \{F_{\phi\theta}\}_e + [K_{\theta\theta}]\{\theta\}_e + \{F_{\theta\theta}\}_e \right) \right) dt = 0 \quad (47)$$

The set of finite element equations for the piezoelectric continuum on the elemental level can be obtained.

$$[M_{uu}]_e \{\ddot{q}\}_e + ([K_L]_e + [K_{NL}]_e - [H_{NL}]_e) \{q\}_e + [K_{u\phi}]_e \{\phi_{p_n}\}_e + [K_{u\theta}]_e \{\theta\}_e = \{F_m\}_e - \{^t_0 F\}_e - \{F_{u\theta}\}_e \quad (48)$$

$$[K_{\phi u}]_e \{q\}_e + [K_{\phi\phi}]_e \{\phi_{p_n}\}_e + [K_{\phi\theta}]_e \{\theta\}_e = \{F_q\}_e - \{F_{\phi u}\}_e - \{F_{\phi\phi}\}_e - \{F_{\phi\theta}\}_e \quad (49)$$

Thereafter, following the classical nonlinear procedure of finite element method of summing over all the elements, the equations obtained in the compact form can be written as

$$\begin{aligned} {}^t_0 [M_{uu}] \{\ddot{q}\} + {}^t_0 [K_{uu}] \{q\} + {}^t_0 [K_{u\phi}] \{\phi\} + {}^t_0 [K_{u\theta}] \{\theta\} &= {}^{t+\Delta t} \{F_m\} - {}^t_0 \{f_{int}\} \\ {}^t_0 [K_{\phi u}] \{q\} + {}^t_0 [K_{\phi\phi}] \{\phi\} + {}^t_0 [K_{\phi\theta}] \{\theta\} &= {}^{t+\Delta t} \{F_q\} - {}^t_0 \{q_{int}\} \end{aligned} \quad (50)$$

Details of the matrices used are given in Appendix.

4 Geometric nonlinear analysis

In the nonlinear case, deformation is large, so the effects of configurational change have to be taken into consideration. The state of equilibrium is obtained if following equation is fulfilled.

$${}^tR - {}^tF_{\text{int}} = 0 \quad (51)$$

where tR is the externally applied nodal point force and ${}^tF_{\text{int}}$ is the nodal point force that corresponds to the elemental stress in the configuration at time ' t '. The equilibrium equation must be satisfied throughout the complete history of load application. This can be effectively carried out using a step-by-step incremental approach as depicted by Bathe (1996). It is assumed that solution for the time ' t ' is known and solution for discrete time ' $t + \Delta t$ ' is required. Hence, at time ' $t + \Delta t$ ' the equilibrium equation is ${}^{t+\Delta t}R - {}^{t+\Delta t}F_{\text{int}} = 0$ when applied to a piezoelectric continuum.

5 Validation and numerical results

5.1 Dynamic validation of simply supported FG plate

A piezolaminated FG plate is considered to validate the natural frequency as a function of the volume fraction for simply supported boundary condition. The results are shown in Table 1. The geometric and material properties used are same as Huang and Shen (2001). The slight difference in the natural frequencies (highest being 9.8%) may be due to different shell theories used for finite element formulation.

Table 1 Natural frequency (Hz) for simply supported FGM plates with actuator layers bonded on the top and bottom surfaces

	Volume fraction						
	0	0.01	0.5	1	5	15	100
He et al. (2001)	144.25	168.74	185.45	198.92	230.46	247.30	259.35
Present linear	151.97	153.32	195.26	216.06	258.55	274.46	276.04
Present nonlinear	149.62	150.98	192.26	218.79	261.96	278.46	279.86

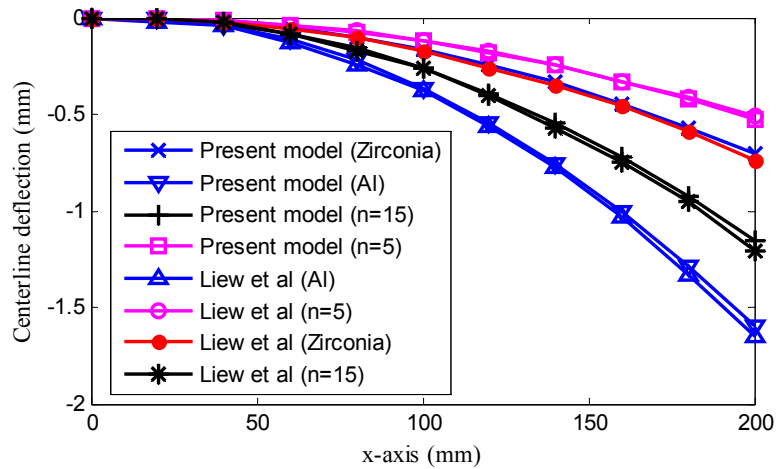
5.2 Validation of functional graded capability under thermal load

A square cantilever FG material plate consisting of combined zirconia and aluminium material constituents with continuously varying mix ratios. The bottom surface of the FGM plate is assumed to be metal rich and the top surface to be ceramic rich. The FGM plate has integrated piezoelectric sensor and actuator patches. The G-1195N piezoelectric patches are bonded to both the top and bottom surfaces of the square plates of length 200 mm and thickness 30 mm. The thickness of the piezoelectric layers is 0.1 mm and the relevant material properties for G-1195N and the aluminium are given in Table 2.

Table 2 Material properties

Properties	Aluminium	Zirconia	G-119N	Ti-6Al-4V
Elastic modulus (N/m ²)	70×10^9	151×10^9	63×10^9	105.70e9
Poisson's ratio	0.3	0.3	0.3	0.2981
Density (Kg/m ³)	2,707	3,000	7,600	4,429
Coefficient of thermal expansion	23×10^{-6}	10×10^{-6}	1.2×10^{-4}	14×10^{-6}
Piezoelectric constant (m/V)			254×10^{-12}	
Dielectric coefficient (F/m)			15×10^{-9}	
Pyroelectric constant (C/m ² k)			0.25×10^{-4}	

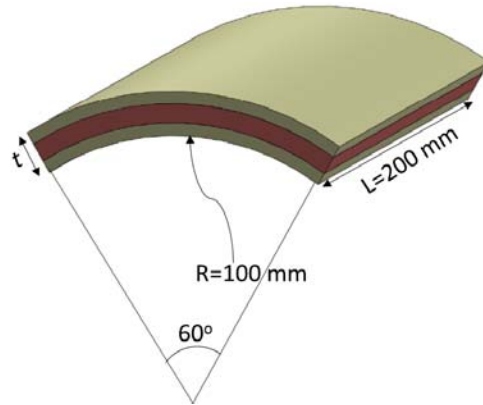
A thermal gradient of 100°C/m is applied to the top surface of the cantilevered square plate and the deflection obtained is in good agreement with referred result of Liew et al. (2001) as shown in Figure 2. In the figure, the centreline deflections of the square plate are shown at various volume fractions. As can be seen from Figure 2 the deflection obtained zirconia is less as compared to aluminium as expected. However, for $n = 5$ the deflection is less than zirconia because the temperature distribution depends on the material properties which leads to smaller deflection.

Figure 2 Centreline deflection along x-axis for FGM plate under thermal gradient of 100°C as presented by Liew et al. (2001) (see online version for colours)

5.3 FGM cylindrical shell

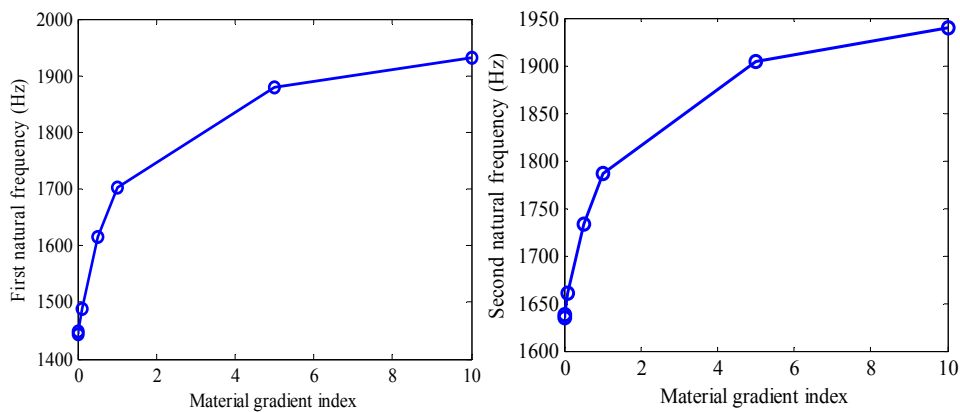
After validating the discussed formulation, a numerical study of large deformation dynamic behaviour of FG piezolaminated cylindrical shell subjected to thermo-electro-mechanical loading is performed. A FG cylindrical shell with 100 mm radius, 200 mm length and the thickness of 1 mm is considered. The angle subtended by cylindrical shell is 60° as shown in Figure 3. The FGM cylindrical shell is composed of zirconia and Ti-6Al-4V and its properties are graded in the thickness direction according to a volume fraction power-law distribution in such a way that bottom surface is ceramic rich and top surface is metal rich. The material properties are given in Table 2.

Figure 3 Piezolaminated functionally graded cylindrical shell presenting geometric dimensions (see online version for colours)

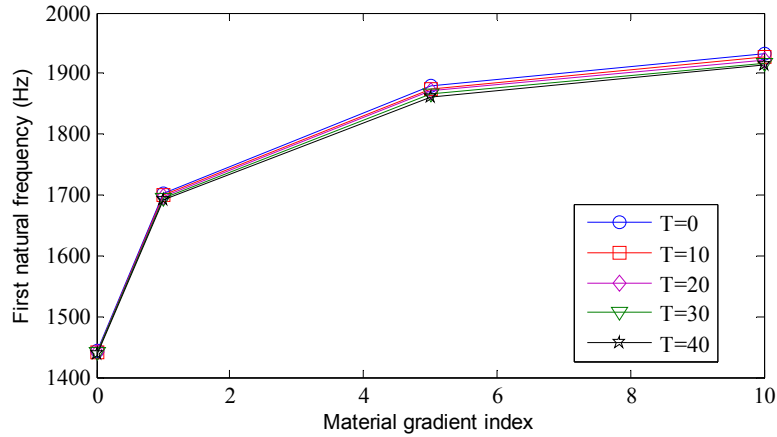
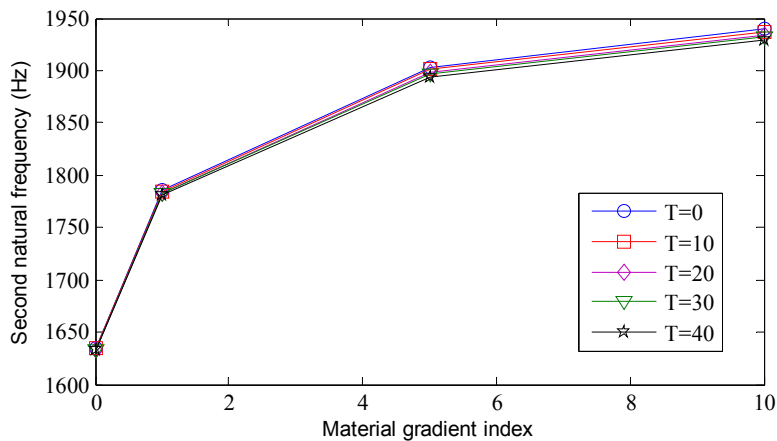


First the effect of material gradient is studied on the natural frequency of the piezolaminated FG cylindrical shell and is shown in Figure 4. As we can see both first and second frequency increases nonlinearly as the material gradient increases from metal rich state to ceramic rich state. This is as expected because metals have low frequency than that of ceramics and as the material gradient and moves towards the ceramic side frequency increases.

Figure 4 Variation of first and second natural frequency with changing material gradients (see online version for colours)



The effect of temperature on the nonlinear frequency behaviour of FG piezolaminated cylindrical shell is also studied at various gradient indexes (0, 1, 5, 10). It can be seen from Figure 5 and Figure 6 as temperature increases the first and second frequency decreases as expected.

Figure 5 Variation of first natural frequency at various temperature gradients (see online version for colours)**Figure 6** Variation of second natural frequency at various temperature gradients (see online version for colours)

Thereafter, the effect of control voltage and thermal environment on the nonlinear vibration analysis of the FG piezolaminated cylindrical shell is studied. In the first case only the effect of temperature is studied and is shown in Table 3 and Table 4 for first two natural frequencies keeping voltage zero. As can be seen from Table 3 and Table 4 the natural frequency decreases nonlinearly as temperature increases. Whereas natural frequency increases with the increase in material gradient. In Table 5 and Table 6, the effect of control voltage can be seen, which shows significant influence on the natural frequency of the structure and by increasing the imposed voltage natural frequency increase in nonlinear manner. It can be seen that the first and second natural frequency of the cylindrical structure increases by increasing the imposed voltage which depicts that by applying appropriate voltage the nonlinear vibration in the structure can be controlled. Also the influence of voltage is higher in the first natural frequency as compared to higher order frequencies which are not that significant in determining the dynamic response of the structure.

Table 3 First natural frequency for various material index and temperature at 0V

Temp/index	0	1	5	10
0	1,442.77	1,703.50	1,879.25	1,932.52
10	1,441.75	1,700.66	1,874.88	1,927.64
20	1,440.72	1,697.83	1,870.54	1,922.79
30	1,439.72	1,695.01	1,866.23	1,917.97
40	1,438.69	1,692.21	1,861.95	1,913.19

Table 4 Second natural frequency for various material index and temperature at 0V

Temp/index	0	1	5	10
0	1,634.63	1,786.20	1,903.38	1,939.68
10	1,634.16	1,784.79	1,901.05	1,937.07
20	1,633.69	1,783.38	1,898.73	1,934.47
30	1,633.24	1,781.99	1,896.43	1,931.90
40	1,632.77	1,780.59	1,894.15	1,929.35

Table 5 First natural frequency for various material index and temperature at 100V

Temp/index	0	1	5	10
0	1,456.84	1,717.74	1,893.57	1,946.88
10	1,558.58	1,821.89	1,999.38	2,053.26
20	1,649.52	1,915.69	2,094.96	2,149.44
30	1,731.89	2,001.03	2,182.11	2,237.18
40	1,807.29	2,079.35	2,262.22	2,317.83

Table 6 Second natural frequency for various material index and temperature at 100V

Temp/index	0	1	5	10
0	1,665.19	1,819.90	1,938.82	1,975.65
10	1,892.37	2,073.35	2,208.81	2,250.90
20	2,095.86	2,298.90	2,448.26	2,494.75
30	2,280.00	2,502.26	2,663.66	2,713.91
40	2,448.24	2,687.53	2,859.57	2,913.13

Table 7 Effect of control voltage, material index and thermal environment on FGM shell

Index	0				1			
	Temp/vol	0	100	200	300	0	100	200
0	1,442.79	1,456.84	1,459.86	1,462.87	1,703.52	1,717.74	1,720.55	1,723.36
10	1,441.76	1,558.58	1,561.28	1,563.96	1,700.68	1,821.89	1,824.44	1,826.97
20	1,440.74	1,649.52	1,651.96	1,654.39	1,697.85	1,915.69	1,918.01	1,920.33
30	1,439.71	1,731.89	1,734.12	1,736.33	1,695.03	2,001.03	2,003.16	2,005.29
40	1,438.68	1,807.29	1,809.35	1,811.39	1,692.23	2,079.35	2,081.34	2,083.31

Table 7 Effect of control voltage, material index and thermal environment on FGM shell (continued)

<i>Index</i>	<i>5</i>				<i>10</i>				
	<i>Temp/vol</i>	<i>0</i>	<i>100</i>	<i>200</i>	<i>300</i>	<i>0</i>	<i>100</i>	<i>200</i>	<i>300</i>
0		1,879.27	1,893.57	1,896.18	1,898.78	1,932.54	1,946.88	1,949.42	1,951.95
10		1,874.90	1,999.38	2,001.74	2,004.11	1,927.66	2,053.26	2,055.57	2,057.87
20		1,870.57	2,094.96	2,097.13	2,099.30	1,922.81	2,149.44	2,151.55	2,153.67
30		1,866.25	2,182.11	2,184.12	2,186.12	1,917.99	2,237.18	2,239.13	2,241.08
40		1,861.97	2,262.22	2,264.08	2,265.93	1,913.21	2,317.83	2,319.65	2,321.46

5.4 *Vibration control of simply supported cylindrical shell*

The vibration control of simply supported piezolaminated FG cylindrical shell subjected to mechanical and thermal loading is also performed. A FG cylindrical shell with 1 m radius, 0.5 m length and the thickness of 1 mm is considered. The angle subtended by cylindrical shell is 85° . The FGM cylindrical shell is composed of zirconia and Ti-6Al-4V. The material properties are given in Table 5. Top layer of piezoelectric material act as sensor and the lower layer as actuator both having the thickness of 0.5 mm each. The voltage generated by sensor is amplified by suitable value and fed back to the actuator which develops a counter balancing force and hence used to control unwanted vibration in the structure. To control the vibrations, due to uniformly distributed mechanical load of 10 KN/m^2 , various controllers such as proportional, derivative and proportional derivative (PD) controller, are used as shown in Figure 7. Vibration control due to thermal gradient of 40°C/m is also presented in this study as shown in Figure 8. Only first vibration mode is targeted as control mode as lower modes of vibration have lower energy associated and can be easily excitable. A time step of 0.0025 sec is considered for transient response of vibrating structure in mechanical and thermal case. No structural damping is considered for both cases. As can be seen from Figure 7 and Figure 8 vibration control is best obtained for PD controller as compared to proportional and derivative controller. The structural vibration is damped approximately by 20.98%, 82.71% and 87.65% in case of mechanical loading after 0.025 sec and in case of thermal loading, by 26.82%, 87.80% and 97.56% after 0.025 sec for proportional, derivative and PD controller respectively.

6 Conclusions

Finite element modelling and analysis have been presented to predict the geometric nonlinear vibration under thermal, electrical and mechanical load. Geometric nonlinear vibrations are damped out using various controllers. Numerical results for various material graded index, temperature and voltages were obtained. Numerical results show that material gradient has significant effect on the natural frequency. Voltage and temperature also affect the natural frequency as well and suggests that voltage can be used to control unwanted vibrations. Mechanical and thermally induced vibrations of FG cylinder are controlled using different controllers. The proportional derivative controller is more effective than other controllers.

Figure 7 Vibration control of FG cylindrical shell using proportional, derivative and PD controller under mechanical loading (see online version for colours)

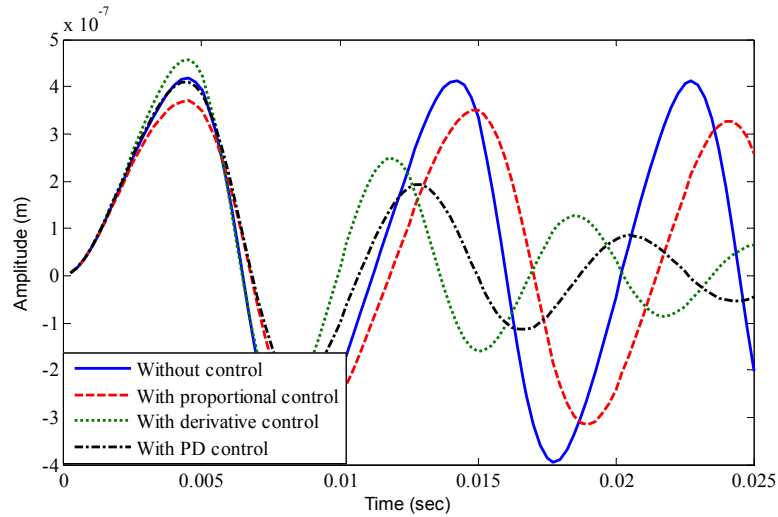
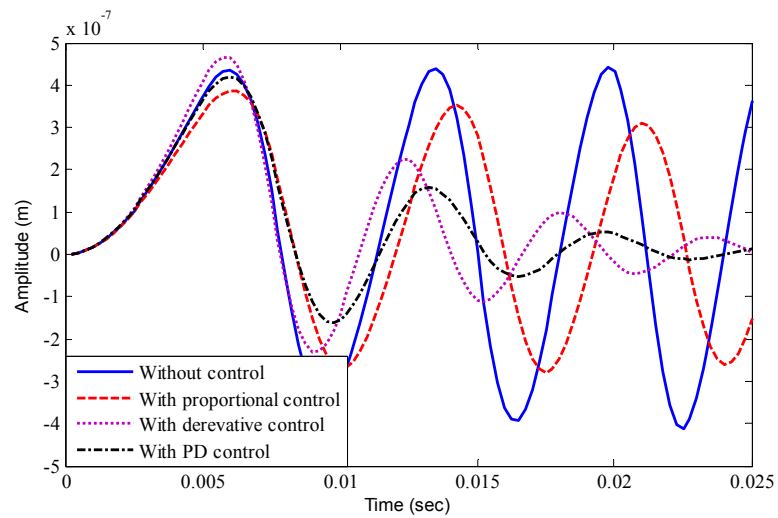


Figure 8 Vibration control FG cylindrical shell using proportional, derivative and PD controller under thermal loading (see online version for colours)



References

- Arciniega, R.A. and Reddy, J.N. (2007) 'Large deformation analysis of functionally graded shells', *International Journal of Solids and Structures*, Vol. 44, No. 6, pp.2036–2052.
- Bathe, K.J. (1996) *Finite Element Procedures in Engineering Analysis*, Prentice-Hall, Englewood Cliffs, NJ.

- Behjat, B. and Khoshhravan, M.R. (2012) 'Geometrically nonlinear static and free vibration analysis of functionally graded piezoelectric plates', *Composite Structures*, Vol. 94, No. 3, pp.874–882.
- Chakraborty, A., Gopalakrishnan, S. and Reddy, J.N. (2003) 'A new beam finite element for the analysis of functionally graded materials', *International Journal of Mechanical Sciences*, Vol. 45, No. 3, pp.519–539.
- Dvorkin, E.N. and Bathe, K.J. (1984) 'A continuum mechanics based four-node shell element for general nonlinear analysis', *Computational Engineering*, Vol. 1, No. 1, pp.77–88.
- Haddadpour, H., Mahmoudkhani, S. and Navazi, H.M. (2007) 'Free vibration analysis of functionally graded cylindrical shells including thermal effects', *Thin-Walled Structures*, Vol. 45, No. 6, pp.591–599.
- He, X., Liew, K.M., Ng, T. and Sivashanker, S. (2002) 'A FEM model for the active control of curved FGM shells using piezoelectric sensor/actuator layers', *International Journal for Numerical Methods in Engineering*, Vol. 54, No. 6, pp.853–870.
- He, X.Q., Ng, T.Y., Sivashanker, S. and Liew, K.M. (2001) 'Active control of FGM plates with integrated piezoelectric sensors and actuators', *International Journal of Solids and Structures*, Vol. 38, No. 9, pp.1641–1655.
- Huang, X. and Shen, H. (2006) 'Vibration and dynamic response of functionally graded plates with piezoelectric actuators in thermal environments', *Journal of Sound and Vibration*, Vol. 289, No. 6, pp.25–53.
- Kordkheili, S.A.H. and Naghdabadi, R. (2007) 'Geometrically non-linear thermoelastic analysis of functionally graded shells using finite element method', *International Journal of Numerical Method in Engineering*, Vol. 72, No. 8, pp.964–986.
- Kumar, R. (2007) *Shape and Vibration Control of Smart Structure*, PhD Thesis, Indian Institute of Technology, Roorkee, India.
- Liew, K.M., He, X.Q., Ng, T.Y. and Sivashanker, S. (2001) 'Active control of FGM plates subjected to a temperature gradient: modelling via finite element method based on FSDT', *International Journal of Numerical Method in Engineering*, Vol. 52, No. 11, pp.1253–1271.
- Qian, L.F., Batra, R.C. and Chen, L.M. (2004) 'Analysis of cylindrical bending thermo-elastic deformations of functionally graded plates by a meshless local Petrov-Galerkin method', *Computational Mechanics*, Vol. 33, No. 4, pp.263–273.
- Reddy, B.S., Suresh Kumar, J., Eswara Reddy, C. and Vijaya Kumar Reddy, K. (2014) 'Free vibration behaviour of functionally graded plates using higher-order shear deformation theory', *Journal of Applied Science and Engineering*, Vol. 17, No. 3, pp.231–241.
- Reddy, J.N. (2000) 'Analysis of functionally graded plates', *International Journal of Numerical Method in Engineering*, Vol. 47, Nos. 1–3, pp.663–684.
- Reddy, J.N., Doshi, S. and Muliana, A. (2011) 'Theoretical formulations for finite element models of functionally graded beams with piezoelectric layers', *Journal of Solid Mechanics*, Vol. 3, No. 4, pp.332–345.
- Tanveer, M. and Singh, A.V. (2010) 'Nonlinear forced vibrations of laminated piezoelectric plates', *Journal of Vibration and Acoustics*, Vol. 132, No. 2, p.021005.
- Uymaz, B. and Aydogdu, M. (2013) 'Three dimensional mechanical buckling of FG plates with general boundary conditions', *Composite Structures*, Vol. 96, pp.174–193.
- Vel, S.S. and Batra, R.C. (2003) 'Three-dimensional analysis of transient thermal stresses in functionally graded plates', *International Journal of Solids and Structures*, Vol. 40, No. 25, pp.7181–7196.
- Woo, J., Meguid, S.A. and Ong, L.S. (2006) 'Nonlinear free vibration behavior of functionally graded plates', *Journal of Sound and Vibration*, Vol. 289, No. 3, pp.595–611.
- Zhao, X. and Liew, K.M. (2009) 'Geometrically nonlinear analysis of functionally graded shells', *International Journal of Mechanical Sciences*, Vol. 51, No. 2, pp.131–144.

Zhao, X., Lee, Y.Y. and Liew, K.M. (2009) ‘Thermoelastic and vibration analysis of functionally graded cylindrical shells’, *International Journal of Mechanical Sciences*, Vol. 51 No. 9, pp.694–707.

Appendix

$$\begin{Bmatrix} S_{11} \\ S_{22} \\ S_{12} \\ S_{13} \\ S_{23} \end{Bmatrix} = \begin{bmatrix} Q_{11} & Q_{12} & 0 & 0 & 0 \\ Q_{21} & Q_{22} & 0 & 0 & 0 \\ 0 & 0 & Q_{66} & 0 & 0 \\ 0 & 0 & 0 & Q_{55} & 0 \\ 0 & 0 & 0 & 0 & Q_{44} \end{bmatrix} \begin{pmatrix} \begin{Bmatrix} \varepsilon_{11} \\ \varepsilon_{22} \\ \varepsilon_{12} \\ \varepsilon_{13} \\ \varepsilon_{23} \end{Bmatrix} - \begin{Bmatrix} 1 \\ 1 \\ 0 \\ 0 \\ 0 \end{Bmatrix} \alpha \theta \\ \begin{Bmatrix} 0 \\ 0 \\ 0 \\ e_{15} \\ 0 \end{Bmatrix} \end{pmatrix} - \begin{bmatrix} 0 & 0 & e_{31} \\ 0 & 0 & e_{32} \\ 0 & 0 & e_{33} \\ e_{15} & 0 & 0 \\ 0 & e_{26} & 0 \end{bmatrix} \begin{Bmatrix} E_1 \\ E_2 \\ E_3 \end{Bmatrix} \quad (A1)$$

$$\begin{Bmatrix} D_1 \\ D_2 \\ D_3 \end{Bmatrix} = \begin{bmatrix} 0 & 0 & 0 & e_{15} & 0 \\ 0 & 0 & 0 & 0 & e_{26} \\ e_{31} & e_{32} & e_{33} & 0 & 0 \end{bmatrix} \begin{pmatrix} \begin{Bmatrix} \varepsilon_{11} \\ \varepsilon_{22} \\ \varepsilon_{12} \\ \varepsilon_{13} \\ \varepsilon_{23} \end{Bmatrix} \\ \begin{bmatrix} b_{11} & 0 & 0 \\ 0 & b_{22} & 0 \\ 0 & 0 & b_{33} \end{bmatrix} \begin{Bmatrix} E_1 \\ E_2 \\ E_3 \end{Bmatrix} - \begin{Bmatrix} 0 \\ 0 \\ P_3 \end{Bmatrix} \end{pmatrix} \theta \quad (A2)$$

$$\begin{aligned}
 \{ {}_0\varepsilon \} = \begin{Bmatrix} {}_0\varepsilon_{xx} \\ {}_0\varepsilon_{yy} \\ {}_0\varepsilon_{zz} \\ {}_0\varepsilon_{xy} \\ {}_0\varepsilon_{zx} \\ {}_0\varepsilon_{yz} \end{Bmatrix} &= \begin{Bmatrix} \frac{\partial_0 u}{\partial_0 x} \\ \frac{\partial_0 v}{\partial_0 y} \\ \frac{\partial_0 w}{\partial_0 z} \\ \frac{1}{2} \left(\frac{\partial_0 u}{\partial_0 y} + \frac{\partial_0 v}{\partial_0 x} \right) \\ \frac{1}{2} \left(\frac{\partial_0 u}{\partial_0 z} + \frac{\partial_0 w}{\partial_0 x} \right) \\ \frac{1}{2} \left(\frac{\partial_0 v}{\partial_0 z} + \frac{\partial_0 w}{\partial_0 y} \right) \end{Bmatrix} \\
 &+ \begin{Bmatrix} \frac{1}{2} \left[\left(\frac{\partial_0 u}{\partial_0 x} \right)^2 + \left(\frac{\partial_0 v}{\partial_0 x} \right)^2 + \left(\frac{\partial_0 w}{\partial_0 x} \right)^2 \right] \\ \frac{1}{2} \left[\left(\frac{\partial_0 u}{\partial_0 y} \right)^2 + \left(\frac{\partial_0 v}{\partial_0 y} \right)^2 + \left(\frac{\partial_0 w}{\partial_0 z} \right)^2 \right] \\ \frac{1}{2} \left[\left(\frac{\partial_0 u}{\partial_0 z} \right)^2 + \left(\frac{\partial_0 v}{\partial_0 z} \right)^2 + \left(\frac{\partial_0 w}{\partial_0 z} \right)^2 \right] \\ \frac{1}{2} \left[\left(\frac{\partial_0 u}{\partial_0 x} + \frac{\partial_0 v}{\partial_0 y} \right) + \left(\frac{\partial_0 v}{\partial_0 x} + \frac{\partial_0 w}{\partial_0 y} \right) + \left(\frac{\partial_0 w}{\partial_0 x} + \frac{\partial_0 v}{\partial_0 y} \right) \right] \\ \frac{1}{2} \left[\left(\frac{\partial_0 u}{\partial_0 x} + \frac{\partial_0 w}{\partial_0 z} \right) + \left(\frac{\partial_0 v}{\partial_0 x} + \frac{\partial_0 w}{\partial_0 z} \right) + \left(\frac{\partial_0 w}{\partial_0 x} + \frac{\partial_0 v}{\partial_0 z} \right) \right] \\ \frac{1}{2} \left[\left(\frac{\partial_0 u}{\partial_0 y} + \frac{\partial_0 w}{\partial_0 z} \right) + \left(\frac{\partial_0 v}{\partial_0 y} + \frac{\partial_0 w}{\partial_0 z} \right) + \left(\frac{\partial_0 w}{\partial_0 y} + \frac{\partial_0 v}{\partial_0 z} \right) \right] \end{Bmatrix} \tag{A3}
 \end{aligned}$$

where

$$\frac{\partial_0 u}{\partial_0 x} = \sum_{k=1}^4 {}_0u_k \frac{\partial h_k}{\partial_0 x} - \alpha_k V_{21}^k g_{x_k} + \beta_k V_{11}^k g_{x_k}$$

$$\frac{\partial_0 v}{\partial_0 y} = \sum_{k=1}^4 {}_0v_k \frac{\partial h_k}{\partial_0 y} - \alpha_k V_{22}^k g_{y_k} + \beta_k V_{12}^k g_{y_k}$$

$$\frac{\partial_0 w}{\partial_0 z} = \sum_{k=1}^4 {}_0w_k \frac{\partial h_k}{\partial_0 z} - \alpha_k V_{23}^k g_{z_k} + \beta_k V_{13}^k g_{z_k}$$

and so on...

$${}^t_0 B_{L0} = \begin{bmatrix} {}_0 h_{k,1} & 0 & 0 & {}^t g_{110}^k G_1^k & {}^t g_{210}^k G_1^k \\ 0 & {}_0 h_{k,2} & 0 & {}^t g_{120}^k G_2^k & {}^t g_{220}^k G_2^k \\ 0 & 0 & {}_0 h_{k,3} & {}^t g_{130}^k G_3^k & {}^t g_{230}^k G_3^k \\ {}_0 h_{k,2} & {}_0 h_{k,1} & 0 & {}^t g_{110}^k G_2^k + {}^t g_{120}^k G_1^k & {}^t g_{210}^k G_2^k + {}^t g_{220}^k G_1^k \\ {}_0 h_{k,3} & 0 & {}_0 h_{k,1} & {}^t g_{110}^k G_3^k + {}^t g_{130}^k G_1^k & {}^t g_{210}^k G_3^k + {}^t g_{230}^k G_1^k \\ 0 & {}_0 h_{k,3} & {}_0 h_{k,2} & {}^t g_{110}^k G_3^k + {}^t g_{130}^k G_2^k & {}^t g_{220}^k G_2^k + {}^t g_{230}^k G_2^k \end{bmatrix} \quad (A4)$$

where

$$g_1^k = -\frac{1}{2} H^0 V_2^k, \quad g_2^k = \frac{1}{2} H^0 V_1^k, \quad {}_0 h_{k,i} = J_{11}^{-1} h_{k,r} + J_{12}^{-1} h_{k,s}$$

and

$${}_0 G_i^k = t \left(J_{11}^{-1} h_{k,r} + J_{12}^{-1} h_{k,s} \right).$$

$${}^t_0 B_{L1} = \begin{bmatrix} l_{11} {}_0 h_{k,1} & l_{21} {}_0 h_{k,1} & l_{31} {}_0 h_{k,1} & {}^t L_{11}^k {}_0 G_1^k & {}^t L_{21}^k {}_0 G_1^k \\ l_{12} {}_0 h_{k,2} & l_{22} {}_0 h_{k,2} & l_{32} {}_0 h_{k,2} & {}^t L_{12}^k {}_0 G_2^k & {}^t L_{22}^k {}_0 G_2^k \\ l_{13} {}_0 h_{k,3} & l_{23} {}_0 h_{k,3} & l_{33} {}_0 h_{k,3} & {}^t L_{13}^k {}_0 G_3^k & {}^t L_{23}^k {}_0 G_3^k \\ l_{11} {}_0 h_{k,2} + l_{12} {}_0 h_{k,1} & l_{21} {}_0 h_{k,2} + l_{22} {}_0 h_{k,1} & l_{31} {}_0 h_{k,2} + l_{32} {}_0 h_{k,1} & {}^t L_{12}^k {}_0 G_2^k + {}^t L_{11}^k {}_0 G_1^k & {}^t L_{21}^k {}_0 G_2^k + {}^t L_{22}^k {}_0 G_1^k \\ l_{12} {}_0 h_{k,3} + l_{13} {}_0 h_{k,1} & l_{21} {}_0 h_{k,3} + l_{23} {}_0 h_{k,1} & l_{31} {}_0 h_{k,3} + l_{33} {}_0 h_{k,1} & {}^t L_{11}^k {}_0 G_3^k + {}^t L_{13}^k {}_0 G_1^k & {}^t L_{21}^k {}_0 G_3^k + {}^t L_{23}^k {}_0 G_1^k \\ l_{12} {}_0 h_{k,3} + l_{13} {}_0 h_{k,2} & l_{22} {}_0 h_{k,3} + l_{23} {}_0 h_{k,2} & l_{32} {}_0 h_{k,3} + l_{33} {}_0 h_{k,2} & {}^t L_{12}^k {}_0 G_3^k + {}^t L_{13}^k {}_0 G_2^k & {}^t L_{22}^k {}_0 G_2^k + {}^t L_{23}^k {}_0 G_2^k \end{bmatrix} \quad (A5)$$

where

$$l_{ij} = \frac{\partial u_i}{\partial x_j} \quad \text{and} \quad L_{ij}^k = \sum_{m=1}^n g_{im}^k l_{mj}.$$

$$\begin{aligned}
{}^0B_{NL} &= \begin{bmatrix}
{}_0h_{k,1} & 0 & 0 & {}^t g_{11}^k G_1^k & {}^t g_{21}^k G_1^k \\
0 & {}_0h_{k,1} & 0 & {}^t g_{12}^k G_1^k & {}^t g_{22}^k G_1^k \\
0 & 0 & {}_0h_{k,1} & {}^t g_{13}^k G_1^k & {}^t g_{23}^k G_1^k \\
{}_0h_{k,2} & 0 & 0 & {}^t g_{11}^k G_2^k & {}^t g_{21}^k G_2^k \\
0 & {}_0h_{k,2} & 0 & {}^t g_{12}^k G_2^k & {}^t g_{22}^k G_2^k \\
0 & 0 & {}_0h_{k,2} & {}^t g_{13}^k G_2^k & {}^t g_{23}^k G_2^k \\
{}_0h_{k,3} & 0 & 0 & {}^t g_{11}^k G_3^k & {}^t g_{21}^k G_3^k \\
0 & {}_0h_{k,3} & 0 & {}^t g_{12}^k G_3^k & {}^t g_{22}^k G_3^k \\
0 & 0 & {}_0h_{k,3} & {}^t g_{13}^k G_3^k & {}^t g_{23}^k G_3^k
\end{bmatrix} \\
[t_\theta]_k &= \begin{bmatrix}
1 & 0 & 0 & 0 & 0 & 0 \\
0 & 1 & 0 & 0 & 0 & 0 \\
0 & 0 & 1 & 0 & 0 & 0 \\
0 & 0 & 0 & V_{11}^k & V_{12}^k & V_{13}^k \\
0 & 0 & 0 & V_{21}^k & V_{22}^k & V_{23}^k \\
0 & 0 & 0 & V_{31}^k & V_{32}^k & V_{33}^k
\end{bmatrix}
\end{aligned} \tag{A6}$$

Thus, the rotational transformation matrix for the four elements may be written as

$$[T_\theta]_e = \begin{bmatrix}
[t_\theta]_1 & 0 & 0 & 0 \\
0 & [t_\theta]_2 & 0 & 0 \\
0 & 0 & [t_\theta]_3 & 0 \\
0 & 0 & 0 & [t_\theta]_4
\end{bmatrix} \tag{A7}$$

The stiffness matrices and force vectors can be defined as

$$\begin{aligned}
{}^0[K_{uu}] &= [K_L]_e + [K_{NL}]_e - [H_{NL}]_e & K_L &= \int_{0V} {}^t B_L^T Q {}^t B_L d^0V \\
K_{NL} &= \int_{0V} {}^t B_{NL}^T Q {}^t B_{NL} d^0V & H_{NL} &= \int_{0V} {}^t B_{NL}^T P {}^t B_{NL} d^0V \\
K_{u\phi} &= \int_{0V} {}^t B_L^T e {}^t B_\phi d^0V & K_{\phi u} &= \int_{0V} {}^t B_\phi^T e {}^t B_L d^0V \\
K_{\phi\phi} &= \int_{0V} {}^t B_\phi^T b {}^t B_\phi d^0V & {}^t \{f_{int_e}\} &= \{ {}^t F \}_e + \{ F_{u\theta} \}_e \\
{}^t \{q_{int_e}\} &= \{ F_{\phi u} \}_e + \{ F_{\phi\phi} \}_e + \{ F_{\phi\theta} \}_e & {}^t F &= \int_{0V} {}^t B_L {}^t \bar{S} d^0V \\
F_{u\theta} &= \int_{0V} {}^t B_L^T \lambda {}^t \theta d^0V & F_{\phi u} &= \int_{0V} {}^t B_\phi^T e {}^t \varepsilon d^0V \\
F_{\phi\phi} &= \int_{0V} {}^t B_\phi^T b {}^t E d^0V & F_{\phi\theta} &= \int_{0V} {}^t B_\phi^T P {}^t \theta d^0V
\end{aligned} \tag{A8}$$